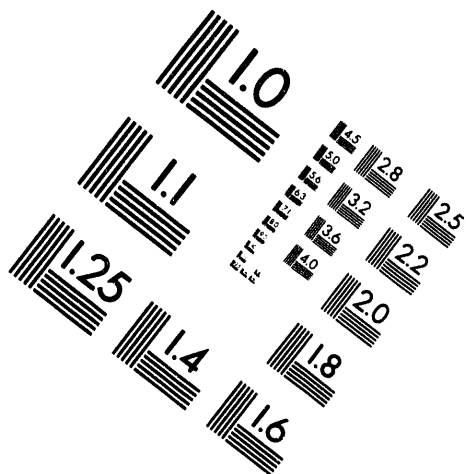
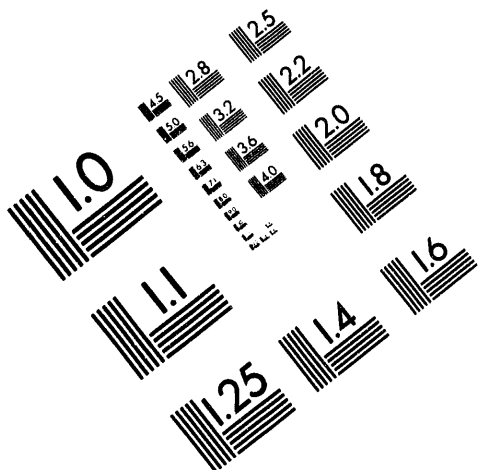




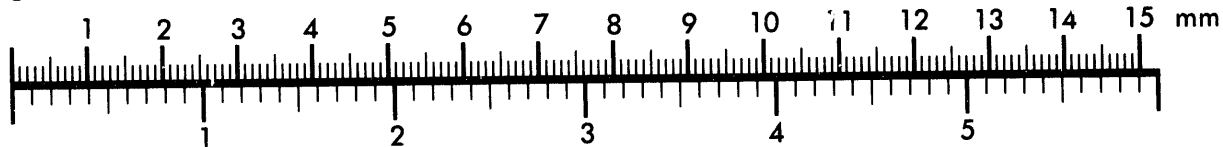
AIM

Association for Information and Image Management

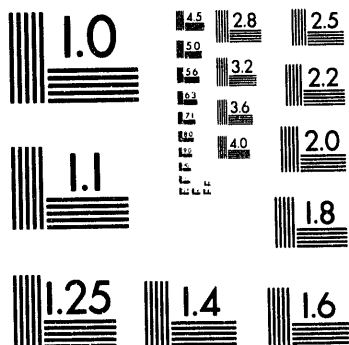
1100 Wayne Avenue, Suite 1100
Silver Spring, Maryland 20910
301/587-8202



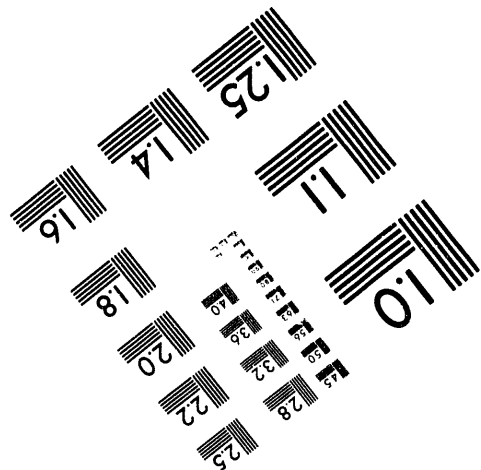
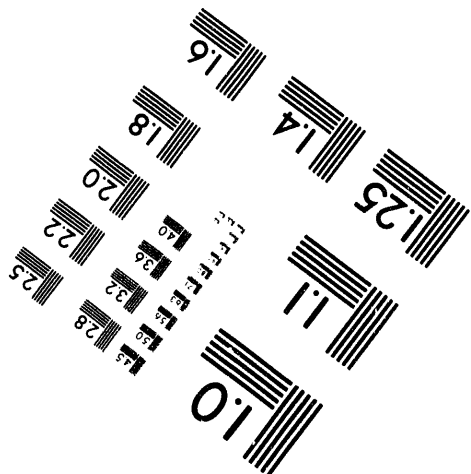
Centimeter



Inches



MANUFACTURED TO AIM STANDARDS
BY APPLIED IMAGE, INC.



1 of 1

BRACING MICRO/MACRO MANIPULATORS CONTROL

J. Y. Lew
W. J. Book^(a)

May 1994

Presented at the
'94 IEEE Robotics and Automation Conference
May 8-12, 1994
San Diego, California

Prepared for
the U.S. Department of Energy
under Contract DE-AC06-76RLO 1830

Pacific Northwest Laboratory
Richland, Washington 99352

(a) Georgia Institute of Technology, Georgia

This report was prepared as an account of work sponsored by an agency of the United States Government. Neither the United States Government nor any agency thereof, nor any of their employees, makes any warranty, express or implied, or assumes any legal liability or responsibility for the accuracy, completeness, or usefulness of any information, apparatus, product, or process disclosed, or represents that its use would not infringe privately owned rights. Reference herein to any specific commercial product, process, or service by trade name, trademark, manufacturer, or otherwise does not necessarily constitute or imply its endorsement, recommendation, or favoring by the United States Government or any agency thereof. The views and opinions of authors expressed herein do not necessarily state or reflect those of the United States Government or any agency thereof.

DISCLAIMER

MASTER

DISTRIBUTION OF THIS DOCUMENT IS UNLIMITED

BRACING MICRO/MACRO MANIPULATORS CONTROL

Jae Young Lew

Automation and Measurement Sciences Department
Pacific Northwest Laboratory*

Wayne J. Book

The George W. Woodruff School of Mechanical Engineering
Georgia Institute of Technology

This paper proposes a bracing strategy for micro/macro manipulators. The bracing micro/macro manipulator can provide advantages in accurate positioning, large work-space, and contact-task capability. However, in exchange for improvement in performance, one must accept the complex control problem along with the complex dynamics. This research develops a control scheme for a bracing manipulator which makes multiple contacts with the environment. Experimental results show the feasibility of the proposed ideas for real world applications.

1. Introduction

In general, a micro arm is mounted on the end of a macro manipulator. The macro manipulator would carry the micro arm to the place of interest in a large work-space. Then, the micro arm would perform fine motions. One of the inherent problems with this serial configuration of micro/macro manipulators is the structural flexibility of the macro manipulator. Bracing a micro/macro manipulator can be one effective way to reduce or damp out its structural vibration. For example, the manipulator would brace against a stationary frame, and the end effector would perform fine motion control just as a human braces the wrist for accurate writing. By forming a close kinematic chain, bracing will stiffen its structure and secure the end point positioning.

Bracing requires a special type of control strategy due to its complex constrained dynamics. This research generalizes the bracing arm control problem as a hybrid control of flexible manipulators with multiple contacts. For example, the end effector works against a workpiece, and the other part of the manipulator may brace against a stationary frame. Then, the manipulator should be able to control the position/force not only at the end effector, but also at the bracing point. This requires hybrid control of multiple contacts with the environment.

This paper presents a hybrid position/force controller for flexible link manipulators which make contact with environment at more than one point. First, a mathematical formulation of the constrained dynamics is obtained. Their dynamics are transformed into two subspaces such as constrained and constraint-free spaces using the singular value decomposition of constraint equations. The force and position controllers are developed based on the orthogonality of these two subspaces. This work has been developed in a generic form for broad application. Theoretical study proves its asymptotic stability, and experimental results show promising feasibility of bracing strategy for real world application.

2. Problem Statement

The bracing arm control problem is generalized to a hybrid control of flexible manipulators with multiple contacts with the environment. Figure 1 shows the general case of a bracing manipulator with n joints, all active, constrained by m contacts with the environment.

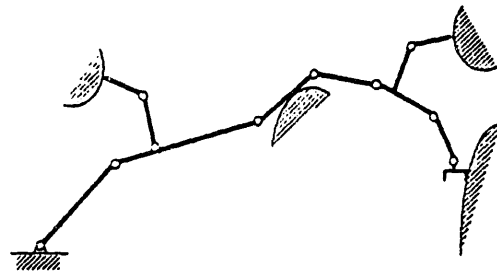


Figure 1 A Flexible Manipulator with Multiple Contact with Environment

The objective is to control the position/force of the end effector while satisfying all the constraints and maintaining desired contact forces at the bracing points. A bracing manipulator, which is a redundant manipulator,

*PNL is operated for the U.S. Department of Energy by Battelle Memorial Institute under Contract DE-AC06-76RLO 1830.

executes the necessary task at the end effector and uses the internal (null) motion to brace at the bracing points. Thus, the task coordinates of the manipulator may be represented as an augmented vector of main task and subtask. For example, the main task is for the end effector to perform the required application, and the subtask is for maintaining bracing forces and positions by internal (null) motion. However, the selection of the subtask requires the following consideration. There should exist a nonsingular Jacobian matrix J , which is the mapping from the active joint coordinates to the task coordinates. This condition is important because it guarantees that the constraints from contact are mutually independent, and each task can be controlled independently by the active joints. Further assumptions are made to formulate the problem:

1. The locations and geometry of constraint surfaces are known in advance. Thus, we can express the constraints with algebraic equations, the so-called configuration constraint equations:

$$\left. \begin{aligned} \phi'_1(x_1) &= \phi_1(q) = 0 \\ \phi'_2(x_2) &= \phi_2(q) = 0 \\ &\vdots \\ \phi'_m(x_m) &= \phi_m(q) = 0 \end{aligned} \right\} m \text{ algebraic equations} \quad (1)$$

where x_i is the position of each contact point in Cartesian surfaces, and q is in the manipulator generalized coordinates.

2. The constraint equations can be written as a set of m constraint surfaces, each of which is assumed to be mutually independent.
3. The manipulator always maintains contacts with the environment while it is in motion.
4. Constraint surfaces are very rigid compared to the manipulator and do not deform due to contact.

3. Dynamics of Bracing Micro/Macro Manipulators

The dynamics of open chain flexible manipulators can be derived using the Lagrangian formulation with the assumed modes method. Also, an efficient method is available for deriving the equations of motion for coupled micro/macro systems. Details can be found in Lew (1993). When a micro/macro manipulator which is flexible, braces against the stationary environment or when the end effector makes contact with the environment, a closed kinematic loop is formed, i.e. the manipulator may make more than one contact. Then, the dynamics of the flexible manipulator will be changed due to the unknown constraint forces from the environment,

and the number of coordinates (system order) will be reduced. This section will formulate the dynamic equations of motion for constrained flexible link manipulators with multiple contact.

One can introduce unknown reaction forces at the contacts between the manipulator and the environment using Lagrange multipliers, and then these reaction forces can be included in the equations of motion as generalized forces. The equations of motion for constrained flexible manipulators due to multiple contact can be represented as:

$$\begin{bmatrix} M_{rr} & M_{rf} \\ M_{fr} & M_{ff} \end{bmatrix} \begin{bmatrix} \ddot{q}_r \\ \ddot{q}_f \end{bmatrix} + \begin{bmatrix} C_{rr} & C_{rf} \\ C_{fr} & C_{ff} \end{bmatrix} \begin{bmatrix} \dot{q}_r \\ \dot{q}_f \end{bmatrix} + \begin{bmatrix} 0 & 0 \\ 0 & k \end{bmatrix} \begin{bmatrix} I \\ b \end{bmatrix} \tau + \phi_1^T \lambda_1 + \phi_2^T \lambda_2 + \dots + \phi_m^T \lambda_m = \begin{bmatrix} I \\ b \end{bmatrix} \tau \quad (2)$$

where

q_r = rigid coordinate such as joint angles for rotational joints, $q_r \in R^r$

q_f = flexible mode amplitude coordinates for each link, $q_f \in R^{n-m}$

M_{ij} = a partition of the inertia matrix of the manipulator. The subscript r denotes rigid, and the subscript f denotes flexible

C_{ij} = a partition of the Coriolis and centrifugal matrix

k = link stiffness matrix

τ = torque from each joint actuator

I = $n \times n$ identity matrix

b = a part of input matrix that relates input torque to flexible mode coordinates. It involves the chosen mode shape functions (assumed modes) and their derivatives evaluated at the boundary.

λ_i = Lagrange multiplier which is the reaction force magnitude at each contact point.

Also,

$$\phi_1 = \frac{\partial \phi_1}{\partial q}, \phi_2 = \frac{\partial \phi_2}{\partial q}, \dots, \phi_m = \frac{\partial \phi_m}{\partial q}$$

where $q = [q_r^T \ q_f^T]^T$. At the same time, the coordinate variables should satisfy the constraint equation (1).

If one combines all of the reaction forces into one matrix and rewrites equation (2) in a simpler form.

$$M\ddot{q} + C\dot{q} + Kq = \phi^T \lambda$$

where

$$\begin{aligned} \phi^T &= [\phi_1^T \ \phi_2^T \ \dots \ \phi_m^T] = \begin{bmatrix} \phi_r^T \\ \phi_f^T \end{bmatrix} \\ \lambda &= [\lambda_1 \ \lambda_2 \ \dots \ \lambda_m]^T \end{aligned}$$

Similarly, we may replace the configuration constraint by a velocity constraint, which is a restriction on the velocity in a specified position. The time derivative of the config-

uration constraint equation, which is the velocity constraint, is:

$$\phi \dot{q} = [\phi_r, \phi_f] \begin{pmatrix} \dot{q}_r \\ \dot{q}_f \end{pmatrix} = 0$$

Recall that $\lambda \in \mathbb{R}^m$ and $\phi^T \in \mathbb{R}^{N \times m}$ and $\text{rank}(\phi^T) = m$ since each constraint is assumed to be independent. Now, we have N ($=$ rigid + flexible) differential equations with m unknowns and m velocity constraints.

4. Hybrid Control for Bracing

4.1 Elimination of Constraint Force (λ)

To design a controller for constrained manipulators, the equation of motion should be represented in a standard form without constraint forces. The constraint forces can be found using Singular Value Decomposition (SVD). The rigid part of the Jacobian constraint matrix, with rank m , can be decomposed into the following form:

$$\phi_r = [u][\Sigma 0] \begin{bmatrix} v_1^T \\ v_2^T \end{bmatrix} \text{ and } \phi_r^T = [v_1 \ v_2] \begin{bmatrix} \Sigma \\ 0 \end{bmatrix} [u^T] \quad (3)$$

where the columns of u are the normalized eigenvectors of the matrix $\phi_r \phi_r^T$. The columns of v_1 are the normalized eigenvectors of the matrix $\phi_r^T \phi_r$, where $v_1 \in \mathbb{R}^{n_r}$ and $v_2 \in \mathbb{R}^{n_f(n-m)}$. Σ is a diagonalized matrix with the square root of non-zero eigenvalues of $\phi_r \phi_r^T$, i.e., $\Sigma = \text{diag}(\sigma_1, \sigma_2, \dots, \sigma_m)$ with $\sigma_1 \geq \sigma_2 \geq \dots \geq \sigma_m$. Detail property of the singular decomposition can be found in Klema (1980), Mani (1985), and Singh (1985). Recall that v_2 is the null space of ϕ_r , which satisfies the following relationship:

$$\phi_r v_2 = 0$$

The reason for taking the SVD of only the rigid part of the constraint matrix is that only rigid joint generalized coordinates have actuators. The actuators generate direct control of the rigid joint angle so that any arbitrary motion can be realized. On the other hand, the flexible generalized coordinates do not have independent actuators in the coordinates. Thus, the flexible motion cannot be controlled independently. The flexible motion is indirectly influenced by the motion of joint angles and the constraint forces. Therefore, it is impossible to generate an orthogonal actuation to all the generalized coordinates.

Now, one transforms the original equations to a new set of differential equations. Let:

$$\bar{v} = \begin{bmatrix} v & 0 \\ 0 & 1 \end{bmatrix} \text{ where } v = [v_1 \ v_2]$$

If we pre-multiply by \bar{v}^T , then the equation of motion becomes:

$$\begin{aligned} \bar{v}^T M \ddot{q} + \bar{v}^T C \dot{q} + \bar{v}^T K q &= \bar{v}^T B \tau + \bar{v}^T \phi^T \lambda \\ &= \bar{v}^T B \tau + \begin{bmatrix} \Sigma u^T \lambda \\ 0 \\ \phi_f^T \lambda \end{bmatrix} \end{aligned} \quad (4)$$

It is seen that the constraint force is eliminated in the second equation corresponding to the zero in the last term of equation (4).

4.2 System Order Reductions

Each configuration constraint equation may be solved for one of the generalized coordinates. Substitution of that result into the equations of motion, and the other constraint equations will remove the selected generalized coordinate from the formulation. The result will be a reduction in the order of the system equations. However, such an approach is effective only for a special form of the algebraic constraints. In this section, the use of the pseudo inverse achieves a systematic reduction of the system order of constrained flexible manipulators.

From constraint equations, we have:

$$\phi \dot{q} = \phi_r \dot{q}_r + \phi_f \dot{q}_f = 0 \quad (5)$$

If one takes the pseudo inverse of the rigid part of the constraint matrix which gives minimum norm, one can obtain an allowable rigid joint motion from the constraint:

$$\dot{q}_r = -\phi_r^+ \phi_f \dot{q}_f + v_2 \dot{z} \quad (6)$$

where $\phi^+ = (\phi \phi^T)^{-1}$. If necessary, one may use weighted pseudo inverse to refine the impact of constraint or to account for different units. The second term of equation (5) gives the null solution for the constraint where v is obtained from the singular value decomposition in equation (3). Equation (5) shows the allowable joint motion which is free from all the constraints. z is any arbitrary vector ($z \in \mathbb{R}^{n-m}$). Eventually, z becomes the new reduced order coordinates. It is difficult to interpret the physical meaning of z for the general case of multiple contacts. However, when the end of the manipulator is constrained, z measures contact point motion which is tangential to the constraint surface.

If we take the time derivative of equation (5) one more time, we can get an acceleration relationship as:

$$\ddot{q}_r = -\phi_r^+ \phi_f \ddot{q}_f + v_2 \ddot{z} + C \quad (7)$$

The integration of equation (6) gives a position relationship:

$$q_r = -\phi_r^+ \phi_f q_f + v_2 z + C \quad (8)$$

Assume that the initial conditions are zero. Thus, $C=0$. Note: In this analysis, the constraint matrix remains constant, i.e., time invariant. This assumption can be

justified if the velocity constraint is obtained as the linearization of the position constraint at an operating point. Only small motions about that operating point are considered here.

Now, the generalized coordinate q_r ($q_r \in \mathbb{R}^m$) may be reduced to new coordinates z ($z \in \mathbb{R}^m$). Substitution of equations (6), (7), and (8) into (4) reduces the order of the system as follows:

$$v_1^T M_{rr} v_2 \ddot{z} + v_1^T (M_{rr} - M_{rr} \phi_r^* \phi_r) \ddot{q}_f + v_1^T C_{rr} v_2 \dot{z} + v_1^T (C_{rr} - C_{rr} \phi_r^* \phi_r) \dot{q}_f = v_1^T \tau + \Sigma u^T \lambda \quad (9)$$

$$v_2^T M_{rr} v_2 \ddot{z} + v_2^T (M_{rr} - M_{rr} \phi_r^* \phi_r) \ddot{q}_f + v_2^T C_{rr} v_2 \dot{z} + v_2^T (C_{rr} - C_{rr} \phi_r^* \phi_r) \dot{q}_f = v_2^T \tau \quad (10)$$

$$M_{ff} v_2 \ddot{z} + (M_{ff} - M_{ff} \phi_r^* \phi_r) \ddot{q}_f + C_{ff} v_2 \dot{z} + (C_{ff} - C_{ff} \phi_r^* \phi_r) \dot{q}_f + K q_f = \phi_f^T \lambda \quad (11)$$

These three sets of differential equations represent the constrained flexible arm dynamics without constraint equations. The first set of equations shows the relationship between constraint forces and arm dynamics. The second set of equations shows the arm's dynamics in the constraint-free space. The third set of equations shows the flexible mode behaviors.

4.3 Quasi-Static Assumptions

Assume that the flexible mode becomes static after bracing, although the joint angles have dynamic motions. Thus, we may assume that terms in equations (9), (10), (11) involving \ddot{q}_f and \dot{q}_f are zero. The justifications of this quasi-static assumption are:

1. Bracing forms kinematic closed loops, consequently, the kinematic structure of the manipulator becomes more rigid.
2. After bracing, the manipulator moves in a relatively slow motion. Therefore, the structural vibration is not excited by the rigid motion of joint angles.

Under the quasi-state condition, the constrained system of dynamic equations (9), (10), and (11) becomes:

$$v_1^T M_{rr} v_2 \ddot{z} + v_1^T C_{rr} v_2 \dot{z} = v_1^T \tau + \Sigma u^T \lambda \quad (12)$$

$$v_2^T M_{rr} v_2 \ddot{z} + v_2^T C_{rr} v_2 \dot{z} = v_2^T \tau \quad (13)$$

$$M_{ff} v_2 \ddot{z} + C_{ff} v_2 \dot{z} + K q_f = \phi_f^T \lambda \quad (14)$$

Based on these quasi-static assumptions, a hybrid controller is proposed and the closed-loop system stability will be investigated.

4.4 Proposed Feedback Controller

The control objective is to make $z \rightarrow z_d$ and $\lambda \rightarrow \lambda_d$. Each contact point should be able to follow the desired trajectory and to maintain the desired contact force. In

this work, we consider only a regulator problem. Let us design a controller as:

$$\tau = v_1 \tau_f + v_2 \tau_p$$

Recall that v_1 and v_2 are orthonormal. Thus, the position control input τ_p does not affect the constrained force dynamics which is represented by equation (12). On the other hand, the force control input τ_f does not effect motion in the constraint-free space, which is shown in equation (13). The matrices v_1 and v_2 work as a kinematic filter to separate the control input into the force controlling input and the position controlling input. The hybrid controller proposed by Raibert (1981) is similar to the proposed controller, and actually is a special case of the proposed controller.

Let the position controller input be:

$$\tau_p = K_p (z_d - z) - K_d \dot{z}$$

where K_p and K_d are the proportional and derivative controller gain matrices. If uncertainty of the system exists, an extra robust controller can be added to guarantee the stability. The detail description can be found in Chen (1989) and Lew (1993). If the proposed position controller is applied to equation (13), it becomes:

$$v_2^T M_{rr} v_2 \ddot{z} + v_2^T C_{rr} v_2 \dot{z} = K_p (z_d - z) - K_d \dot{z}$$

The solution of the state z is asymptotically stable as long as K_p and K_d are positive definite. In other words, z converges to a constant desired state z_d . This can be proved by using the Lyapunov analysis and the Invariant Set Theorem since the matrix $M_{rr} - 2C_{rr}$ is skew symmetric.

Recall that the response of the system differential equations has to satisfy equations (12), (13), and (14). If the state z is controlled to be the desired state z_d by the position controller, \dot{z} and \ddot{z} become zero at steady state. Then, equation (12) becomes an algebraic equation as:

$$\tau_f = -\Sigma u \lambda + K_f (\lambda - \lambda_d)$$

Let the force controller input be:

$$\tau_f = -\Sigma u \lambda + K_f (\lambda - \lambda_d)$$

where K_f is the force controller gain. Thus, the position controller τ_p should be able to make $z \rightarrow z_d$ and at the same time, the force controller will make $\lambda \rightarrow \lambda_d$ with the proposed force control input. On the other hand, the magnitude of the flexible mode becomes:

$$q_f = K^{-1} \phi_f^T \lambda_d$$

To represent the control input in terms of joint angles and flexible modes which are measurable, multiply the equations (6) and (8) by v_1^T . We can obtain:

$$\dot{z} = v_2^T \dot{q}_r - v_2^T \dot{\phi}_r^* \dot{\phi}_f$$

$$z = v_2^T q_r - v_2^T \phi_r^* \phi_f$$

Since the bracing arm dynamics is assumed to be quasi-static, \dot{q}_r is zero. Thus the control input is:

$$\tau = v_1 \{-\sum u_i \lambda + K(\lambda_d - \lambda)\}$$

$$+ v_2 [-K_d v_2^T \dot{q}_r + K_p \{z_d - v_2^T (q_r - \phi_r^* \phi_f)\}]$$

5. Experimental Case Study

A large experimental arm designated RALF (Robotic Arm, Large and Flexible) has been constructed and is under computer control. RALF consists of two links, each being ten feet long and approximately five inches in diameter. At the tip of RALF, SAM (Small Articulated Arm) with a bracing foot is mounted as shown in Figure 2. SAM also has two links, and the length of each link is about two feet.

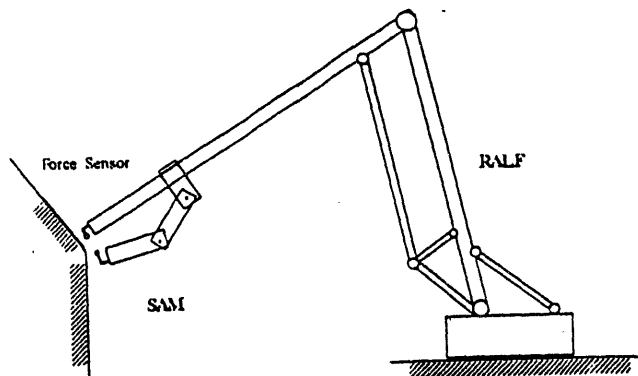


Figure 2 Experimental Apparatus of RALF and SAM for Hybrid Control

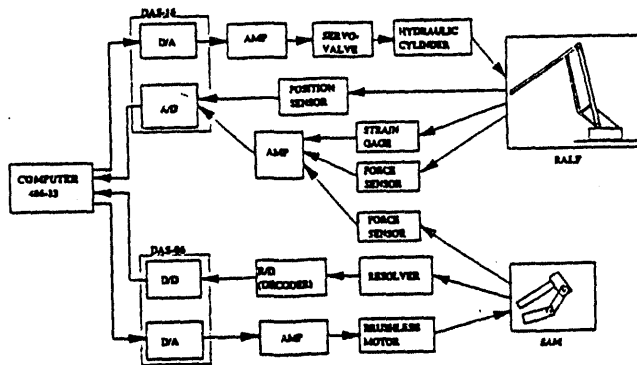


Figure 3 RALF and SAM Controller Architecture

Figure 3 shows the controller architecture. Both the arms are controlled by a PC 486-33 with two A/D boards. The program is written in C language, and the sampling rate for experiments was set at 4 msec. Two "custom-

made" force sensors are used to measure the contact forces, and the strain gages at each link of RALF give the information of how much the link deflects.

5.1 Single Contact Point Hybrid Control

The proposed hybrid control is applied to a single end-point contact case. The experiment is carried out using only RALF. The constraint surface is located 11 feet away from the base of RALF and has a slope of 125 degrees as shown in Figure 2. The tip of RALF moves very close to the constraint surface using PD position control. That position corresponds to each joint angle at 105 degrees. Then RALF performs force control against the surface and follows a desired trajectory along the surface. The desired force is 1.5 lbf, and the trajectory is given as a cycloidal motion for one foot of travel distance.

Figure 4(a) and (b) show the experimental results. Figure 4(a) shows the relatively good tracking motion of the tip of RALF along the constraint surface. The plot of the tip position is computed from the measured joint angles. The switch from the PD position control mode to the hybrid control mode causes the initial jump in the motion as shown in Figure 4(a). Figure 4(b) shows the contact force measured by the force sensor at the tip of RALF. The high frequency oscillation of the measured force at the start of the motion is due to the structural vibration of the force sensor. After contact at 3.7 sec, the contact force follows the desired force as we expected. Still, there exists significant steady state error in contact force, but this error may be reduced by adding an integral term of the force error to the force controller.

5.2 Two Point Contact (Bracing) Hybrid Control

A second experiment will be performed to show two point hybrid control. The bracing foot of RALF is to brace against the same constraint surface as in the previous experiment, and the tip of SAM also makes a contact with a vertical constraint surface as shown in Figure 2. Two arms carry out the proposed multiple contact hybrid control against two different surfaces.

The second task is to move RALF and SAM while bracing. While RALF performs the bracing strategy, SAM executes the hybrid motion control. Figure 5(a) shows the force measurement at the bracing point. Similar to the previous case, the force controller takes a long time to settle down and has a large overshoot, but the response converges to the desired force eventually.

Figure 5(b) shows the trajectory tracking of SAM along the vertical constraint surface. The goal is to follow a cycloidal trajectory; however, again, the response was poor due to noise from the brushless motor and the coupling dynamics between the two arms. Improvement

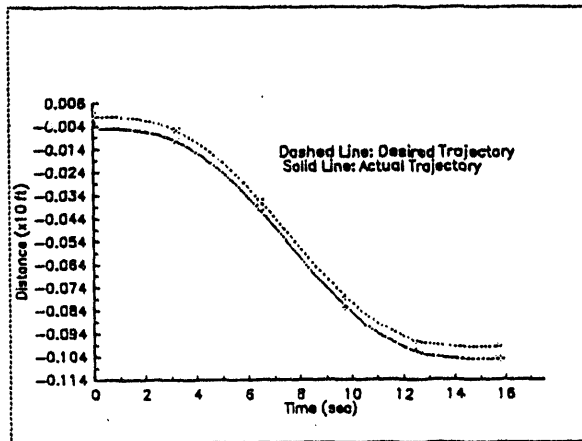


Figure 4(a) RALF Position Control along the Constraint Surface

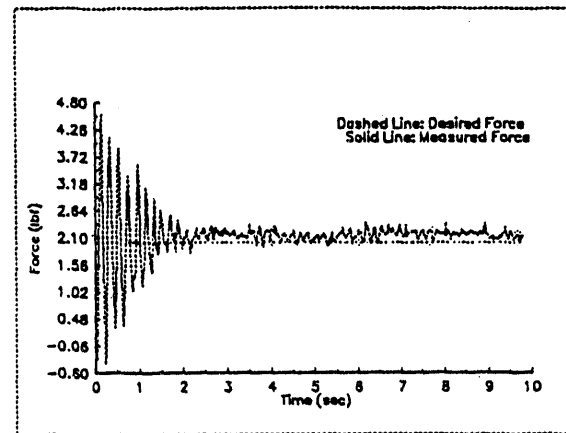


Figure 5(a) RALF Bracing Force Measurement while SAM's Hybrid Motion

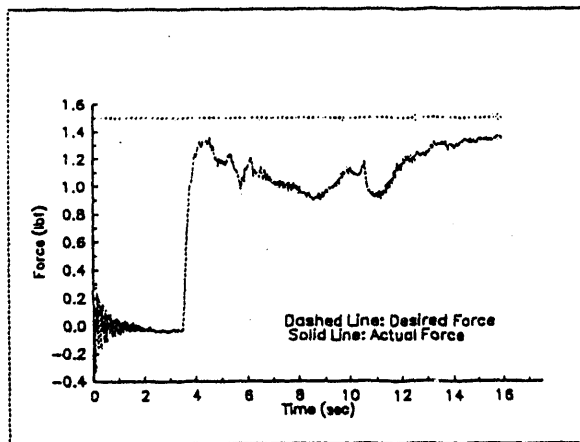


Figure 4(b) RALF Force Control against the Constraint Surface

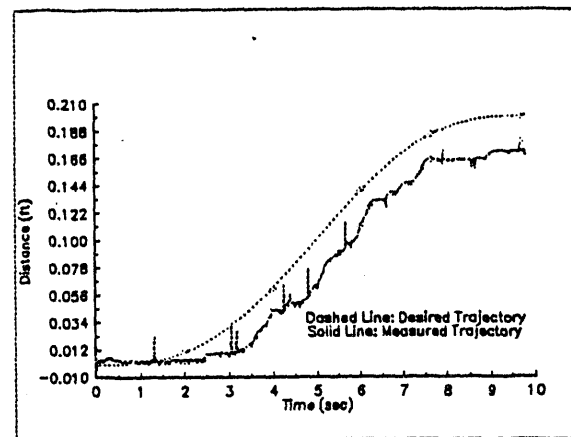


Figure 5(b) SAM Tip Motion along the Constraint Surface while RALF Bracing

may be achieved by more sophisticated servo controllers. Figure 5(c) shows SAM's controlled force measurement against the constraint surface. The contact force converges to the desired force slowly. Since the force controller is operated mainly under static information, its response is relatively slow compared to the position controller response. When two force control routines are applied at the same time for each manipulator, the total system force response is diminished significantly.

5.3 Effectiveness of Bracing RALF

One of the main reasons to brace a large flexible manipulator is to reduce its structural vibration. In this experiment, we investigate how much vibration is actually reduced by bracing. This time, RALF carries SAM at the tip and braces with a bracing foot against the stationary frame. RALF applies hybrid control to maintain the constraint force and bracing position, while SAM performs a circular motion. An accelerometer is mounted at

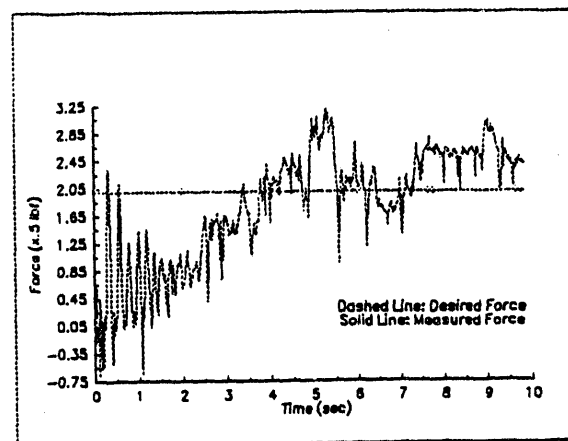


Figure 5(c) SAM Contact Force Measurement while RALF Bracing

the tip of RALF and measures the structural vibration to examine the effectiveness of the bracing strategy.

An HP signal analyzer is used to compute the power spectrum of the accelerometer signal. As shown in Figure 6, the lowest structural frequency is observed at 2.6 Hz, and the second one at 3.3 Hz without bracing. Bracing makes the first peak of vibration smaller by 13 db and the second peak shifts to 4.1 Hz. This phenomenon can be explained as a change of boundary conditions. Without bracing, the boundary condition of the open chain structure is a free condition, but with bracing, the closed chain structure more closely resembles a pin condition. Thus, bracing causes faster and smaller amplitude structural vibration.

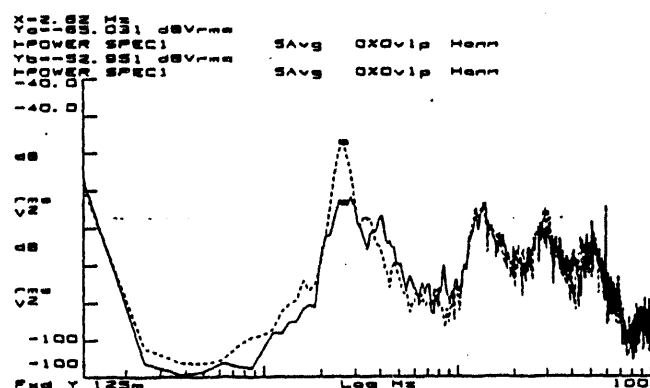


Figure 6 Power Spectrum of RALF End Point Acceleration Measurement (dashed line: without bracing, solid line: with bracing)

6. Conclusion

A hybrid controller is developed for flexible link manipulators which make contact with the environment at more than one point. The controller is derived under the general case of multiple contact constrained dynamics. Using singular value decomposition of a constraint matrix, the control input torque is divided to achieve position and force control in each direction. The stability of the proposed hybrid controller is proved analytically. An experimental study carries out the implementation of the proposed hybrid control for the prototype micro/macro manipulators, RALF and SAM. Under various task conditions, the proposed real-time controller accomplishes tracking position control along the constraint surface and force control against the surface. A bracing strategy is realized to show its feasibility for real world applications. The relative comparison study of effectiveness of bracing is carried out and shows the reduction of vibration in an arbitrary configuration.

Acknowledgments

This work was partially supported by the U.S. Department of Energy Robotics Technology Development Program, Sandia National Laboratory Contract 18-4379G, and NASA Grant NAG1-623.

References

- Book, W., Le, S. and Sangveraphunsiri, "The Bracing Strategy for Robot Operations," The 5th Symposium on Theory and Practice of Robots and Manipulator, Udine, Italy, 1984.
- Chen, Y.H. and Pandey, S., "Robust Hybrid Control of Robot Manipulators," in Proc. 1989 IEEE International Conference on Robotics and Automation, pp. 235-241, Scottsdale, Arizona, April 1989.
- Fisher, W.D. and Mujitaba, M.S., "Sufficient Stability Condition for Hybrid Position Force Control," in Proc. 1992 IEEE International Conference on Robotics and Automation, pp. 1336-1341, Nice, France, May 1992.
- Klema, V.C. and Laub, A.J., "The Singular Value Decomposition; Its Computation and Some Applications," IEEE Transaction on Automatic Control, April 1980, pp. 164-176.
- Lew, J. and Book, W., "Control of Two Cooperative Disparate Manipulators," Fourth Topical Meeting on Robotics and Remote System, Albuquerque, New Mexico, February 1991.
- Lew, J., "Control of Bracing Micro/Macro Manipulator," Ph.D. Thesis, Dept. of Mechanical Engineering, George Institute of Technology, February 1993.
- Mani, N.K., Haug, E.J., and Atkinson, K.E., "Application of Singular Value Decomposition for Analysis of Mechanical System Dynamics," ASME Journal of Mechanics, Transmissions, and Automation in Design, March 1985, pp. 82-87.
- Mason, M., "Compliance and Force Control for Computer Controlled Manipulators," IEEE Transaction System, Man and Cybernetics, Vol. SMC-1, No. 6, pp. 418-432, 1981.
- McClamroch, N. and Wang, D., "Feedback Stabilization and Tracking of Constrained Robots," in Proc. American Control Conference, pp. 464-469, Minneapolis, Minnesota, 1987.
- Mills, J., "Hybrid Control: A Constrained Motion Perspective," Journal of Robotic Systems, pp. 135-158, 1991.
- Raibert, M. and Craig, J., "Hybrid Position/Force Control of Manipulators," ASME Journal of Dynamics, System, Measurement, and Control, Vol. 102, pp. 126-131, 1981.
- Singh, R. and Lipkins, P., "Singular Value Decomposition for Constrained Dynamical Systems," Journal of Applied Mechanics, Vol. 52, December 1985.
- West, H. and Asada, H., "A Method for the Design of Hybrid Position/Force Controllers for Manipulators Constrained By Contact With the Environment," in Proc. IEEE Robotics and Automation Conference, St. Louis, Missouri, 1985.
- Yoshikawa, T., Sugie, T., and Tanaka, T., "Dynamic Hybrid Position/Force Control of Robot Manipulators-Controller Design and Experiment," in Proc. IEEE Robotics and Automation Conference, pp. 2005-2010, Raleigh, North Carolina, 1987.

**DATE
FILMED**

8/11/94

END

